Quantitative evaluation of Compressed Sensing in MRI: application to 7T time-of-flight angiography

Julien Milles, Maarten J. Versluis, Andrew G. Webb and Johan H.C. Reiber, *Fellow, IEEE*

***Abstract*—Compressed Sensing is a recently developed technique that enables the reconstruction of sparsely sampled MR data, thus enabling much faster image acquisitions than using conventional approaches which are limited by the Nyquist criterion. Even though this method has been shown to provide visually acceptable results in a number of applications, no quantitative evaluation of the quality of the image data reconstructed using this method have yet been provided. In this paper we evaluate Compressed Sensing reconstruction in terms of sensitivity to its intrinsic reconstruction parameters as well as to the acquisition strategy both with simulated and experimental time-of-flight angiography data acquired on a 7T clinical MR scanner. Results show that Compressed Sensing reconstruction outperforms traditional methods of undersampling such as simple zero-filling and provides data with acceptable quality at undersampling rates up to a factor of ten. Such an acquisition framework therefore appears to be a valid and promising approach for reducing data acquisition time.**

I. Introduction

CURRENT trends in clinical medical imaging are to minimize data acquisition times for a particular imaging modality while keeping image quality as high as possible. In the case of magnetic resonance imaging (MRI), this can, for example, be achieved using techniques such as parallel imaging [1,2]. Recently, a technique based on the seminal work by Candès on Compressive Sampling [3,4] has been developed under the name of Compressed Sensing (CS) [5], showing very encouraging results when applied to MR data acquisition [6]. This technique is based on the principle that when k-space is undersampled using a random sampling pattern, incoherent artifacts are generated that can be corrected for by the spatial redundancy of MR. It presents the significant advantage of being potentially usable with any MR scanner without any specific hardware equipment.

The inherent reduction in acquisition time using such acceleration techniques can be used to reduce the total time spent in the scanner by the patient with resolution and coverage kept constant, to increase the spatial resolution of the image, or to increase the volume that is covered at a given spatial resolution.

CS has been used in an increasingly wide range of MR applications such as lung imaging [7], localized spectroscopy [8], velocity imaging [9] and catheter visualization [10]. Combination of CS with parallel imaging techniques has also been explored [11]. However, to our knowledge very little work has been put in the quantitative evaluation of the actual accuracy achieved using such compressive techniques, besides the study by Miao and colleagues using data acquired with Compressed Sensing to evaluate their perceptual difference model [12]. As a result, there is no indication to what speed-up factor would be realistically applicable in the clinic.

In this study, we evaluate the stability and accuracy of CS applied to time-of-flight (TOF) angiography scans acquired from a 7T MRI human scanner. TOF angiography is a very natural application of high field MRI, taking advantage of the lengthened T1 values of tissue for improved suppression of background tissue. Isotropic spatial resolutions of less than 0.25x0.25x0.25 mm^3 have already been achieved. Angiographic data appear to be a very natural data type for which CS can be used, as the spatial support of information is inherently sparse. In the next section, we shortly describe compressed sensing and its implementation on a clinical scanner. Section III describes the evaluation methodology and the acquired data. Results are subsequently presented and discussed, before the concluding remarks.

II. Compressed sensing

A. Principles

Compressed sensing originates form Information and Approximation Theory. In that framework, one measures a limited number of random linear combinations of signal values, without maintaining the Nyquist sampling criterion, and reconstructs the original signal using a nonlinear constrained reconstruction. Three conditions have to be fulfilled for CS to be applicable:

- the desired signal has a sparse representation in a known transform domain.
- the artifacts due to undersampling are incoherent in that transform domain.
- a nonlinear reconstruction can be used to enforce both the sparsity of the image representation in the transformed domain and consistency with the acquired data.

In the case of angiographic MR images, the sampled linear coefficients are Fourier coefficients originating from the k-space data, and the reconstruction is based on a trade-off between piecewise continuity, the sparse transform being finite differences, and agreement with samples, as described in the following section.

Manuscript received July 15, 2010.

J. Milles and J.H.C. Reiber are with the Division of Image Processing, Department of Radiology, Leiden University Medical Center, Leiden, the Netherlands (corresponding author J. Milles: +31-715-265-342; fax: +31-715-266-801; e-mail: J.R.Milles@lumc.nl;J.H.C.Reiber@lumc.nl).

M.J. Versluis and A.G. Webb are with the CJ Gorter center for high field MRI, Department of Radiology, Leiden University Medical Center, Leiden, the Netherlands (e-mail: M.J.Versluis@lumc.nl; A.G.Webb@lumc.nl).

978-1-4244-6561-3/10/$26.00 ©2010 IEEE

B. Implementation of Compressed Sensing

Implementation of CS in a clinical setting necessitates generating a random sampling pattern in k-space as well as implementing the constrained reconstruction algorithm. Those two points are described in the following subsections.

1) Random sampling

In order to achieve a sampling scheme random enough to result in incoherent artifacts and thus a near-optimal solution, we chose to use a Monte-Carlo based procedure. We first build a probability density function (pdf) with the desired shape and subsequently randomly draw samples locations according to that pdf.

In the case of MR data, it is desirable to choose a pdf with a higher probability at the center of the k-space, so that more points are drawn where most of the information is located. Once a sampling pattern has been determined, it can be used again for subsequent scans.

2) Image reconstruction

In this section, we will describe the processes of non-linear image reconstruction. Let I be the image of interest, Ψ the linear operator so that $\Psi\ I$ is sparse and F_u the undersampled Fourier transform corresponding to the k-space undersampling described in the previous section. The image reconstruction process can be written as a set of two equations, one promoting sparsity and the other enforcing data consistency. Sparsity is ensured by minimizing

$$\|\Psi I\|_1 + \alpha TV(I) \quad (1)$$

where $\|x\|_1 = \sum_i |x_i|$ is the L1 norm and TV the total variation of the image, meaning the sum of the finite differences in the image, according to [12]. The parameter α is used to vary the relative weights given to each of the terms. Data consistency is classically defined as

$$\|F_u I - y\|_2 < \varepsilon \quad (2)$$

with $\|x\|_2 = (\sum_i |x_i|^2)^{1/2}$ being the euclidian L2 norm. This set of equations is solved iteratively during reconstruction.

III. Evaluation Methodology

A. Evaluation strategy

The strategy is designed to keep our evaluation methodology as application-independent as possible, focusing on the accuracy of the reconstructed data. The methodology is divided into two stages. First, the sensitivity and stability of the CS reconstruction algorithm is evaluated. For that purpose, we use data acquired with complete k-space sampling which is subsequently artificially subsampled, referred to as simulated Compressed Sensing (simulated CS). Simulated CS allows varying the original sampling pattern as well as the total variation term in order to test the stability of the reconstruction algorithm with regard to those parameters. Reconstruction accuracy can also be studied in the same way.

Subsequently, experimental data were actually acquired with a subsampled k-space and used to evaluate the accuracy of CS reconstruction and compare it to traditional zero-filled reconstruction of the undersampled data. CS reconstruction based on actual subsampled data is further referred to as experimental Compressed Sensing (experimental CS). Both evaluation methods are described in the following subsection, as well as the data acquired for evaluation purposes.

B. Simulated Compressed Sensing

1) Sensitivity to the sampling pattern

As described in the previous section, the acquisition of CS data relies on the definition of a subsampled acquisition pattern. That sampling pattern is obtained by randomly drawing samples according to a user-defined pdf in a Monte-Carlo framework. Before evaluating the accuracy of the data obtained for a larger range of values, we evaluated the sensitivity of the reconstruction to that random drawing process by reconstructing data obtained from different patterns at constant subsampling rate. The accuracy of the obtained reconstruction is then measured using the Normalized Mean-Square Error (NMSE) and compared to that of classic zero-filled (ZF) reconstruction.

2) Effects of the total variation term:

In a similar fashion as the sensitivity to the sampling pattern mentioned above, we evaluate the influence of the weighting parameter for total variation. The reconstruction error in terms of NMSE is evaluated for an α value ranging from 0, no total variation weighting, to 10, heavily variation weighted.

3) Reconstruction accuracy

Reconstruction accuracy was evaluated by computing the NMSE for both the original data and Maximum Intensity Projection (MIP) images, as the latter are the most common method of visualizing and assessing angiography data. The MIP volume was constructed by computing 36 projections obtained by rotating the data with 10 degrees steps around the z (foot-head) axis.

C. Experimental Compressed Sensing

Data obtained from experimental CS were evaluated qualitatively by displaying MIP images and quantitatively in terms of reconstruction accuracy, using the same framework as the one described in Section II.A.3, by computing the NMSE for both the original data and MIP images.

D. Evaluation data

Evaluation data consisted of time-of-flight angiography datasets covering the whole head of a healthy volunteer. Data were acquired using a Philips 7T clinical scanner and a quadrature head coil. Four volumes were scanned, corresponding to k-space sampling of 100%, 50%, 30% and 10% respectively, during the same session. K-space points were obtained directly from the scanner as list/data format, Philips' proprietary format for raw data. Each volume was 512x256x128 in size, with a resolution of 1x1x1 mm^3. Acquisition time was 9 minutes for the fully sampled dataset, acquisition time decreasing linearly with sampling rate. The relatively low spatial resolution chosen was due to the need to acquire fully sampled data for evaluation purposes.

IV. Results and Discussion

A. Simulated Compressed Sensing

1) Sensitivity to the sampling pattern

According to the methodology presented in Section III.A.1, we generated 10 reconstructions with 10 different computed undersampling masks, all originating from the same pdf and designed to generate a sampling pattern covering 25% of the k-space. The average NMSE computed between each of those reconstructed volumes and the original, fully sampled, volume was 0.35±0.07 for CS reconstruction and 1.37±0.08 for ZF reconstruction. This demonstrates that CS reconstruction is fairly stable with regard to the sampling pattern when keeping the sampling rate constant and that it performs better than ZF reconstruction for such a low sampling rate.

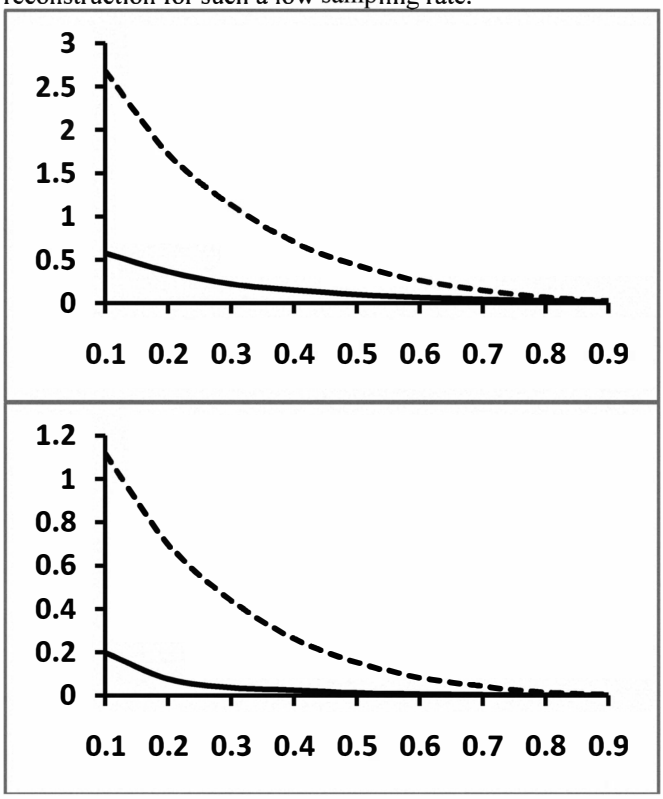

Fig. 1. NMSE as a function of k-space sampling fraction for simulated CS. The top plot corresponds to image data, and the bottom to MIP data. Dotted lines correspond to ZF reconstruction and solid lines to CS reconstruction. An indication of standard deviation is provided in Section IV.A.1.

2) Effects of the total variation term

We evaluated the quality of reconstruction, by means of NMSE, for *TV* weights varying between 0 and 10 and a sampling percentage of 25%, similarly to the previous experiment. The value 0 yielded a NMSE of 1.42, showing the importance of having a term limiting total variation within the image, but for the other values, integers ranging from 1 to 10 with increments of 1, yielded an average NMSE of 0.3±0.03.

3) Reconstruction accuracy

Results of the sampling rate on the reconstruction accuracy is shown in Figure 1. As could be predicted, the NMSE decreases when sampling rate increases for both ZF and CS reconstructions and for both image and MIP data. One can however observe that the error inherent with CS reconstruction is much lower than that obtained with ZF reconstruction, especially for the lowest sampling rates. Reconstruction errors observed for MIP data are much lower for both reconstruction strategies, which can be explained by the fact that by definition MIP data emphasize the influence of high intensity structures, such as in our case the vasculature, limiting the influence of spurious local variations. However, it is interesting to note that the measured NMSE for image data reconstructed with CS is actually lower than the NMSE measured for MIP data reconstructed with ZF.

B. Experimental Compressed Sensing

Examples of MIP images obtained from the data acquired with experimental CS are shown in Figures 2 and 3. Figure 2 shows that ZF reconstruction suffers greatly from subsampling on two accounts. First, the contrast between the vasculature and other brain tissues diminishes strongly. Secondly, the vasculature itself loses its sharpness and small vessels, such as the ones to the right of the top image, are disappearing.

ome degradation can be observed in Figure 3, which shows ıe same data reconstructed with CS: the fading of the maller vessels can also be observed, although less ramatically. However, the contrast between vasculature and ther brain tissues is preserved by the sparsity constraint. hese results were numerically confirmed, as the NMSE orresponded to the values predicted by simulated CS for oth image and MIP data.

Fig. 2. Example of MIP images computed from data reconstructed with the traditional Zero-Filling algorithm. From top to bottom: 100%, 50%, 30% and 10% k-space sampling respectively. The dynamic range for each image was normalized.

V. Discussion

In this paper, we studied the stability of CS reconstruction with regard to the sampling pattern and reconstruction constraints, as well as the accuracy of CS reconstruction compared to ZF, in the case of angiographic data. We should note, however, that the data we acquired were of relatively low resolution since the acquisition of a fully sampled dataset, with a long scan duration, was limiting the attainable resolution. This limiting factor was all the more important that we chose to use a quadrature volume transmit/receive coil rather than a multi-channel phased array receive configuration. The reason for such a choice was that we wanted to isolate any possible confounding effect, such as the additional use of parallel imaging. Since the stability and accuracy of CS reconstruction has been demonstrated, our future directions will involve the combination both Compressed Sensing and parallel imaging techniques in order to obtain higher acceleration factors and realistic measurement times for clinical studies.

Secondly, we limited our study to one main parameter, NMSE, and did not make use of more sophisticated post-processing method in order to evaluate, for example, segmentation accuracy. As we mentioned in Section III, we were aiming at providing an application-independent outlook on the stability and accuracy of CS reconstruction. Segmentation being by definition application-specific, introduces several other factors into the quantitative evaluation of the end product. Further studies should however consider these aspects as well, together with te effects of pathology on the method.

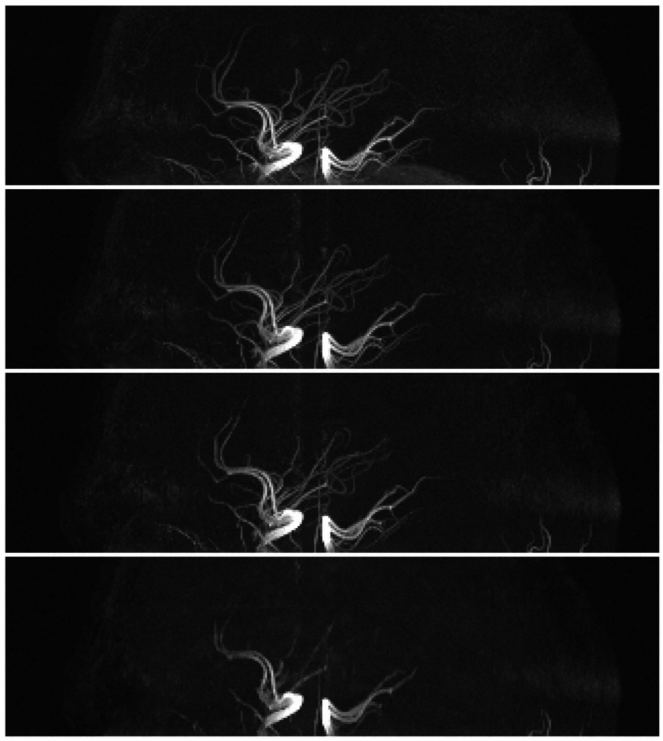

Fig. 3. Example of MIP images computed from data reconstructed with Compressed Sensing. From top to bottom: 100%, 50%, 30% and 10% k-space sampling respectively. The dynamic range for each image was normalized.

VI. Conclusion

We evaluated Compressed Sensing reconstruction accuracy using both simulated and actually implemented techniques. Results show that CS reconstruction is stable with regard to the choice of sampling pattern, at constant sampling rate, and that the presence of a Total Variation term in the sparsity constraint greatly enhances the results.

Regarding the actual implementation of the CS reconstruction, we showed that reasonable results could be obtained, with CS constantly outperforming traditional ZF reconstruction.

References

[1] D.K. Sodickson and W.J. Manning, "Simultaneous acquisition of spatial harmonics (SMASH): Fast imaging with radiofrequency coil arrays," *Magn. Reson. Med.*, vol. 38, pp.591–603, 1997.

[2] K.P. Pruessmann, M. Weiger, M.B. Scheidegger and P. Boesiger, "SENSE: Sensitivity encoding for fast MRI," *Magn. Reson. Med.*, vol. 42, pp. 952–962, 1999.

[3] E. Candès, J. Romberg and T. Tao, "Tobust uncertainty principles: Exact signal reconstruction from highly incomplete frequency information," *IEEE Trans. Inf. Theory*, vol. 52, pp. 489-509, 2006.

[4] E.J. Candès and M.B. Wakin, "An introduction to Compressive Sampling,," IEEE Signal Proc Mag, vol. 25, pp. 21-30, 2008.

[5] D. Donoho, "Compressed sensing," *IEEE Trans. Inf. Theory*, vol. 52, pp. 1289-1306, 2006.

[6] M. Lustig, D. Donoho and J.M. Pauly, "Sparse MRI: The application of Compressed Sensing for rapid MR imaging," *Magn. Reson. Med.*, vol. 58, pp. 1182-1195, 2007.

[7] S. Ajraoui, K.J. Lee, M.H. Deppe, S.R. Parnell, J. Parra-Robles and J.M. Wild, "Compressed sensing in hyperpolarized 3He lung MRI," *Magn. Reson. Med.*, vol. 63, pp. 1059-1069, 2010.

[8] S. Hu, M. Lustig, A. Balakrishnan, P.E. Larson, R. Bok, J. Kurhanewicz, S.J. nelson, A. Goga, J.M. Pauly and D.B. Vigneron, "3D compressed sensing for highly accelerated hyperpolarized (13)C MRSI with in vivo applications to transgenic mouse models of cancer," *Magn. Reson. Med.*, vol. 63, pp. 312-321, 2010.

[9] D.J. Holland, D.M. Malioutov, A. Blake, A.J. Sederman and L.F. Gladden, "Reducing data acquisition times in phase-encoded velocity imaging using compressed sensing," *J. Magn. Reson.*, vol. 203, pp. 236-246, 2010.

[10] C.O. Schirra, S. Weiss, S. Krueger, D. Caulfield, S.F. Pedersen, R. Razavi, S. Kozerke and T. Schaeffer, "Accelerated 3D catheter visualization from triplanar MR projection images," *Magn. Reson. Med.*, vol. 64, pp. 167-176, 2010.

[11] H. Jung, J. Park, J. Yoo and J.C. Ye, "Accelerating SENSE using compressed sensing," *Magn. Reson. Med.*, vol. 62, pp. 1574-1584, 2009.

[12] J. Miao, F. Huang, D.L. Wilson, " Comprehensive quantitative image quality evaluation of compressed sensing MRI reconstructions using a weighted perceptual difference model (Case-PDM): selective evaluation, disturbance calibration, and aggregative evaluation of oise, blur, aliasing, and oil-painting artifacts", in *Proc. SPIE*, Vol. 7627, pp. 762709-762713, 2010.

[13] Y. Tsaig and D.L. Donoho, "Extensions of compressed sensing," *Signal Process.*, vol. 86, pp. 533-548, 2006.